

Networks of non-equilibrium condensates for global optimization

Kirill P. Kalinin¹ and Natalia G. Berloff^{2,1*}

¹*Department of Applied Mathematics and Theoretical Physics,
University of Cambridge, Cambridge CB3 0WA, United Kingdom and*

²*Skolkovo Institute of Science and Technology Novaya St.,
100, Skolkovo 143025, Russian Federation*

(Dated: 10 August 2018)

Abstract

Recently several gain-dissipative platforms based on the networks of optical parametric oscillators, lasers and various non-equilibrium Bose–Einstein condensates have been proposed and realised as analogue Hamiltonian simulators for solving large-scale hard optimisation problems. However, in these realisations the parameters of the problem depend on the node occupancies that are not known *a priori*, which limits the applicability of the gain-dissipative simulators to the classes of problems easily solvable by classical computations. We show how to overcome this difficulty and formulate the principles of operation of such simulators for solving the NP-hard large-scale optimisation problems such as constant modulus continuous quadratic optimisation and quadratic binary optimisation for any general matrix. To solve such problems any gain-dissipative simulator has to implement a feedback mechanism for the dynamical adjustment of the gain and coupling strengths.

*correspondence address: N.G.Berloff@damtp.cam.ac.uk

In the last five years we have seen the rapid emergence of a new field at the intersection of laser and condensed matter physics, engineering and complexity theories which aims to develop quantum devices to simulate classical spin problems faster than on classical von Neumann architecture using a gain-dissipative principle of operation. If the simulated spin problem is NP-hard, then solving it efficiently opens a new route for solving many practically relevant NP problems [1]. Certainly, solving such problems by any physical means would require the number of operations that grows exponentially fast with the size of the problem (the ‘NP-hardness assumption’ [2]), but finding the ways to solve these problems for a fixed problem size faster than by a classical Turing machine has a considerable practical importance. Among such strongly NP-hard problems are finding the global minimum of the Ising and XY Hamiltonians [3], for which even an approximate solution is hard to find [4]. Several platforms were proposed and demonstrated as a proof-of-principle for finding the global minimum of such spin Hamiltonians: injection-locked laser systems [5], the networks of optical parametric oscillators, [6–9], coupled lasers [10], polariton condensates [11], and photon condensates [12]. The main principle of such simulators is based on a gain process that raises the system above the threshold for a phase transition to a coherent state (a Bose-Einstein condensate, laser coherence, synchronisation of oscillators, etc.). Since the threshold is first reached at the state that maximises the occupation for a given pumping intensity, this state is related to a ground state of a particular spin Hamiltonian [11, 13].

Such Hamiltonians are written for N classical ‘spins’ $\mathbf{s}_j = (\cos \theta_j, \sin \theta_j)$. In the XY model ‘spins’ are continuous, whereas for the Ising model the ‘spins’ take discrete values as the phases θ_j are restricted to 0 or π . The ‘spins’ are coupled to each other with the ‘strengths’ J_{ij} that can be positive (ferromagnetic) or negative (antiferromagnetic), so that at the ground state ‘spins’ arrange their orientation as to minimise $H = -\sum_{i=1}^N \sum_{j=1}^N J_{ij} \cos(\theta_i - \theta_j)$. Finding the global minimum of the Ising or XY Hamiltonians are also known as the quadratic binary optimisation and constant modulus quadratic continuous optimisation problems, respectively.

In the gain-dissipative simulators the ‘spin’ – the node (the ‘bit’) of the simulators – is represented by the phase of a condensate at a particular spatial position [11, 12] or by the phase of a coherent state generated in a laser cavity [9, 10], so by the phase of the so-called *coherent center* (CC). All of the proposals to use the gain-dissipative simulators to find the absolute minimum of the spin Hamiltonians suffer from a serious limitation. As

we show below, the coupling strengths J_{ij} in such systems are modified by the occupations (number densities) of CCs i and j . The densities, however, are not known *a priori* and, for a general matrix \mathbf{J} will be different from one CC to another. The density inhomogeneity may also lead to the system fragmentation when different subsystems acquire their own mode of oscillation, and the coherent steady state across all CCs will never be reached. In all the previous experimental realisations of the gain-dissipative simulators, an explicit or implicit assumption was made that the coupling terms are small so that each laser or condensate is stabilised independently at the same steady-state amplitude [5, 6, 9–11]. Such assumption is justified only for the simplest structures of the coupling matrix \mathbf{J} , where all CCs are almost equally connected with about the same coupling strengths. The found solution for a more general matrix is bound to be either only approximate or invalid. The problem of unequal densities has been recognised before [14], but the proposed method to reduce the heterogeneity in densities was to drive the system using randomly modulated signals and can yield only very modest improvement and only if the densities are quite close for the unmodulated signals.

In this paper we formulate the technological requirements for gain-dissipative platforms to be used as analogue Hamiltonian optimisers. We develop a general framework for the operation of the gain-dissipative analogue simulators based on the Langevin gain-dissipative equations written for a set of CCs. We derive the rate equations for the geometrically coupled CCs such as in polariton or photon condensates. We show that by establishing a feedback connection between the gain mechanism and the density of the CC we can drive the system to the coherent ground state of the XY model, while the minimisers of this ground state will give the true minimum precisely for the externally provided coupling strengths. This framework allows us to formulate the hardware requirements for a physical realisation of any such simulator to achieve such a minimum and argue that such requirements are within the recent technological capabilities.

The operation of a gain-dissipative simulator consists of two stages: bosonic stimulation below the threshold and the coherence of operations at and above the threshold. As one ramps up the power of the gain mechanism (e.g. laser intensity) the gain overcomes the linear losses and is stabilised by the nonlinear gain saturation. The emergent coherent state maximises the total number of particles (minimises losses) and, therefore, minimises the Ising or XY Hamiltonian depending on whether the phases of the CCs are discrete or continuous,

respectively. To derive the governing equations for the system one can describe each CC at a position $\mathbf{r} = \mathbf{r}_i$ by a classical complex function $\Psi_i(t)$. Depending on the system, the couplings K_{ij} between CCs can have a different origin: they can be geometrically induced by the particle outflow from other CCs [11] or induced by the mutual injection rate between lasers [9, 15] or spatially separated condensates; they can be controlled by external potentials [12]. In what follows we derive the rate equations for the CCs in the geometrically induced flow in the network of non-equilibrium condensates (such as e.g. polariton or photon condensates) starting from the mean-field description by the complex Ginzburg-Landau equation (cGLE) [16, 17]. The CC in this case is the wavefunction of an individual condensate in the lattice where the spatial degree of freedom has been integrated out. Such mathematical elimination of the spatial degree of freedom has been done before [18] using the infinite quantum well orthogonal basis. We are interested in the time evolution of the complex amplitudes describing the individual condensates in the lattice; therefore, we will use a non-orthogonal basis associated with the wavefunction of an individual condensate. The cGLE [16] is a driven-dissipative equation of non-equilibrium condensates that has been extensively used to model the steady states, spatial pattern formation and dynamics of polariton condensates (for review see [19, 20]). It can be written as

$$i\frac{\partial\psi}{\partial t} = -\nabla^2\psi + (\tilde{U} - i\tilde{\sigma})|\psi|^2\psi + i\left(\sum_{i=1}^N P(|\mathbf{r} - \mathbf{r}_i|)f_i(t) - \gamma_c\right)\psi, \quad (1)$$

where $\psi(\mathbf{r}, t)$ is the wavefunction of the system, \tilde{U} is the strength of the delta-function interaction potential, the sum on the right-hand side represents the rate of adding particles in N spatial locations $\mathbf{r} = \mathbf{r}_i$, $i = 1, \dots, N$, $P_i(\mathbf{r}) \equiv P(|\mathbf{r} - \mathbf{r}_i|)$ is a given spatially localised pumping profile, that creates the condensate with a wavefunction $\phi_i(\mathbf{r}) = \phi(|\mathbf{r} - \mathbf{r}_i|)$ centred at $\mathbf{r} = \mathbf{r}_i$ with a normalised number density so that $2\pi \int |\phi(r)|^2 r dr = 1$. Furthermore, f_i is the time-dependent part of the pumping at $\mathbf{r} = \mathbf{r}_i$, γ_c is the rate of linear losses and $\tilde{\sigma}$ is the rate of the density-dependent losses. In writing Eq. (1) we let $\hbar = 1$ and $m = 1/2$. If the distances between CCs are larger than the width of $P(r)$, the wavefunction of the condensate can be written as $\psi(\mathbf{r}, t) \approx \sum_{i=1}^N a_i(t)\phi_i(\mathbf{r})$ [21], where $a_i(t)$ is the time-dependent complex amplitude. We substitute the expression for ψ into Eq. (1), multiply by ϕ_j^* for $j = 1, \dots, N$,

and integrate in space to yield the rate equations for $a_j(t)$

$$i\dot{\mathbf{a}}^T = \left[-\mathbf{D} + i\mathbf{\Gamma} - i\gamma_c\mathbf{\Xi} + (\tilde{U} - i\tilde{\sigma})\mathbf{Q} \right] \mathbf{a}^T \mathbf{\Xi}^{-1}, \quad (2)$$

where $\mathbf{a} = \{a_i\}$, $\mathbf{\Xi} = \{\chi_{ij}\}$, $\mathbf{D} = \{d_{ij}\}$, $\mathbf{\Gamma} = \{\Gamma_{ij}\}$, $\mathbf{Q} = \{q_{ij}\}$, and $\chi_{ij} = \int \phi_i \phi_j^* d\mathbf{r}$, $q_{ij} = \int |\sum_{k=1}^N a_k \phi_k|^2 \phi_i \phi_j^* d\mathbf{r}$, $\Gamma_{ij} = \sum_k f_k \int P_k \phi_i \phi_j^* d\mathbf{r}$, and $d_{ij} \equiv \int \phi_j^* \nabla^2 \phi_i d\mathbf{r}$. An asymptotics of $\phi(r)$ for the Gaussian pumping profile have been developed in [21] where we showed that function ϕ can be approximated by

$$\phi(r) = \sqrt{\frac{2}{\pi}} \beta \exp[-\beta r + ik_c r], \quad (3)$$

where k_c is the outflow velocity and β is the inverse characteristic width of the condensate [21]. The integrals $\chi_{ij} = \int \phi_i \phi_j^* d\mathbf{r}$ for $i \neq j$ can be evaluated in elliptical coordinates in terms of the Bessel functions [22]

$$\chi_{ij} = 2\beta^2 l_{ij} \left[\frac{1}{\beta} J_0(k_c l_{ij}) K_1(\beta l_{ij}) + \frac{1}{k_c} J_1(k_c l_{ij}) K_0(\beta l_{ij}) \right], \quad (4)$$

where $l_{ij} = |\mathbf{r}_i - \mathbf{r}_j|$. We assumed that the CCs are well separated: $l_{ij}\beta \gg 1$, so that for $i \neq j$ we have $\chi_{ij} \ll 1$ as follows from Eq. (4). The integrals in the off-diagonal terms in \mathbf{Q} are of the same order in smallness as χ_{ij} . Below the threshold $a_i(t) = 0$ and at the threshold $|a_i(t)|^2$ are non-zero but small (polaritons are bosons and therefore obey the Bose-Einstein statistics at low densities characterised by $a_i(t)$). The off-diagonal terms in \mathbf{Q} are quadratic in these small quantities and can be neglected to the linear order in Eq. (2), so that \mathbf{Q} is the diagonal matrix with elements $|a_i|^2 q$, where $q = 2\pi \int |\phi|^4 r dr$. One can show that $d_{ij} \ll d_{ii}$ and can be neglected to the linear order, so that $\mathbf{D} = d\mathbf{I}$, where $d = 2\pi \int \phi \nabla^2 \phi r dr$. The matrix $\mathbf{\Xi}$ has 1 on the diagonal and χ_{ij} as ij -th element. Taking the inverse and keeping only up to the linear order terms gives a matrix with 1 on the diagonal and $-\chi_{ij}$ as the ij -th element. Finally, to the linear order terms the elements of matrix $\mathbf{\Gamma}$ are $\Gamma_{ii} = f_i p$ and $\Gamma_{ij} = (f_i p_{ij} + f_j p_{ji}^*)$ for $i \neq j$, where $p = 2\pi \int P(r) |\phi|^2 r dr$, and $p_{ij} = \int P_i \phi_i \phi_j^* d\mathbf{r}$. To the linear order terms in small quantities $|a_i(t)|^2$ and p_{ij} and neglecting $\chi_{ij} \ll p_{ij}$ for $i \neq j$ Eqs.

(2) become

$$\frac{d\Psi_i}{dt} = \Psi_i(\gamma_i^{\text{inj}} - \gamma_c - (iU + \sigma)|\Psi_i|^2) + \sum_{j,j \neq i}^N \Delta_{ij}^{\text{inj}} K_{ij} \Psi_j + D\xi_i(t), \quad (5)$$

where we used the quadratic smallness of $p_{ij} - p_{ji}^*$, let $\Psi_i = a_i \exp(i\omega t)$, $\gamma_i^{\text{inj}} = f_i p$, $U = q\tilde{U}$, $\sigma = q\tilde{\sigma}$, $K_{ij} = \text{Re}\{p_{ij}\}/p$, $\Delta_{ij}^{\text{inj}} = \gamma_i^{\text{inj}}(t) + \gamma_j^{\text{inj}}(t)$ and introduced the Langevin noise $\xi_i(t)$ ($\langle \xi_i(t)\xi_i^*(t') \rangle = \delta(t - t')$) which represents intrinsic vacuum fluctuations and classical noise with a diffusion coefficient D which disappears at the threshold. In other platforms such as the Coherent Ising Machines [6] the injection does not have to be symmetric between the nodes – this will be modelled by introducing an asymmetry parameter δ so that $\Delta_{ij} = \gamma_i^{\text{inj}}(t) + (1 - \delta)\gamma_j^{\text{inj}}(t)$, where $\delta = 0$ for symmetrically coupled CCs. Equations (5) are the rate equations on the CCs coupled with the strengths $\Delta_{ij}K_{ij}$. Note, that by writing the coupling strength in this form we separated the effect of what is not known a priori (pumping intensity, energy at the threshold etc) from K_{ij} that depends on the characteristics of the system that are known and for geometrically coupled condensate, for instance, depend on the distance between CCs i and j . To show how Eqs. (5) lead to the XY model minimisation we rewrite them in terms of the number densities ρ_i and phases θ_i using the Madelung transformation $\Psi_i = \sqrt{\rho_i} \exp[i\theta_i]$ while suppressing noise:

$$\frac{1}{2}\dot{\rho}_i(t) = (\gamma_i - \sigma\rho_i)\rho_i + \sum_{j:j \neq i} \Delta_{ij}^{\text{inj}} K_{ij} \sqrt{\rho_i\rho_j} \cos \theta_{ij}, \quad (6)$$

$$\dot{\theta}_i(t) = -U\rho_i - \sum_{j:j \neq i} \Delta_{ij}^{\text{inj}} K_{ij} \frac{\sqrt{\rho_j}}{\sqrt{\rho_i}} \sin \theta_{ij}, \quad (7)$$

where $\theta_{ij} = \theta_i - \theta_j$. The first term on the right-hand side of Eq. (7) tends to provide θ_i with its own frequency of oscillations whereas the second term couples the phases to each other and so tends to synchronise them, in the full analogy with the Kuramoto model that Eq. 7 represents [23]. The phase synchronisation in this context assumes the constant (but not necessarily zero) phase differences between the CCs. Phase synchronisation in such a system has been extensively studied especially in the context of semiconductor laser arrays [24, 25]. To guarantee that the steady state of the system is reached and coincides with a minimum of the XY model, however, one needs to ensure that the gain mechanism is chosen so that all densities ρ_i are the same at the steady state at the threshold. Only under

this condition does the second term on the right-hand side of Eq. (7) describe the gradient decent to the minimum of the XY model. Previously, any realisation of the XY model using the laser systems (or non-equilibrium condensates) was based on the assumption that all lasers (condensates) have the same steady-state photon (particle) number [9, 24, 25]. This limits the problems that can be addressed by such a framework to trivial ones where all CCs have an almost equal number of connections with almost the same pumping rate. Different densities at the threshold even if the steady state and therefore phase synchronisation is achieved imply that although the system reached the minimum of the XY Hamiltonian the coupling coefficients $\Delta_{ij}^{\text{inj}} K_{ij}$ are replaced by $\Delta_{ij}^{\text{inj}} K_{ij} \sqrt{\rho_j/\rho_i}$ where ρ_i and ρ_j are not known *a priori*. To implement any couplings and connectivities, one needs to be able to control the pumping rate of the individual CCs and bring all the densities to the same value at the threshold, so that the term $\sqrt{\rho_j/\rho_i}$ is cancelled out. We schematically illustrate the operational principle of such control mechanism in Fig. 1a. Starting from below the threshold, all CCs are equally pumped as shown at some $t = t_1$. Depending on the node connectivity, the non-zero densities emerge at different rates for each CC as the pumping intensity increases and takes some CCs above the specified threshold $\rho = \rho_{\text{th}}$ as illustrated on Fig. 1a at some later time $t = t_2$. The pumping mechanism must be adjusted for each CC to enable the saturation at the same density: decreased for CCs with densities above the threshold and increased for the CCs below the threshold. The feedback mechanism can be implemented via optical delay lines (in a network of optical parametric oscillators system), by adjusting the injection via the spatial light modulator (SLM) (in the polariton and photon condensates) or by electrical injection (e.g. in the polariton lattices [30]). The mathematical description of such a feedback mechanism is

$$\frac{d\gamma_i^{\text{inj}}}{dt} = \epsilon(\rho_{\text{th}} - \rho_i), \quad (8)$$

where ϵ is a parameter that can be tuned to control the speed of approaching the threshold. The fixed point of Eqs. (6-8) is $\rho_i = \rho_{\text{th}} = (\gamma_i^{\text{inj}} - \gamma_c + \sum_{j;j \neq i} \Delta_{ij}^{\text{inj}} K_{ij} \cos \theta_{ij})/\sigma$, with the total particle number given by $M = (\sum_i \gamma_i^{\text{inj}} - N\gamma_c + \sum_{i,j;j \neq i} \Delta_{ij}^{\text{inj}} K_{ij} \cos \theta_{ij})/\sigma$. Since the pumping of each of the CCs is controlled independently from the others by gradually increasing the gain from below until the threshold density value is achieved, the condensation will first take place at the minimum of $\sum_i \gamma_i^{\text{inj}}$ for a given set of coupling coefficients. Since $M = N\rho_{\text{th}}$ and

$N\gamma_c$ are fixed, the minimum of $\sum_i \gamma_i^{\text{inj}}$ is achieved at the maximum of $\sum_{i,j;j \neq i} \Delta_{ij}^{\text{inj}} K_{ij} \cos \theta_{ij}$ so at the minimum of the XY Hamiltonian $H_{XY} = -\sum_{i,j;j \neq i} \Delta_{ij}^{\text{inj}} K_{ij} \cos \theta_{ij}$. The minimum is approached from below by gradually raising the pumping to the threshold which facilitates the achievement of the global minimum as Fig. 1a at $t = t_3$ illustrates.

In the context of the cGLE appropriate for the description of non-equilibrium condensates the nonlinear dissipation σ can be proportional to the pumping intensity $\sigma = c\gamma_i^{\text{inj}}$ [19], where c is a system dependent parameter that for polariton condensates for instance depends on the decay rate of the particles in the hot exciton reservoir. The steady state of Eqs. (6-8) becomes $\rho_i = \rho_{\text{th}} = (1 - \gamma_c/\gamma_i^{\text{inj}} + \sum_{j;j \neq i} \Delta_{ij}^{\text{inj}} K_{ij} \cos \theta_{ij})/c$, with $\Delta_{ij}^{\text{inj}} = 1 + \gamma_j^{\text{inj}}/\gamma_i^{\text{inj}}$. In this case, at the threshold each of $1/\gamma_i^{\text{inj}}$ (and so $\sum_i 1/\gamma_i^{\text{inj}}$) is maximised, so again the system reaches the minimum of the XY Hamiltonian.

If one removes the density heterogeneity the global minimum of the XY model will be achieved, but the coupling terms $\Delta_{ij}^{\text{inj}}(t)K_{ij}$ now depend on the particle injection rates γ_i^{inj} that would not be known *a priori* if one requested the equal densities at the threshold. Therefore, not only $\gamma_i^{\text{inj}}(t)$ has to be adjusted in time to equalise the densities using Eq. (8) but also the coupling parameters K_{ij} have to be modified in time to bring the required couplings J_{ij} at the steady state by

$$\frac{dK_{ij}}{dt} = \hat{\epsilon}(J_{ij} - \Delta_{ij}^{\text{inj}}K_{ij}), \quad (9)$$

where $\hat{\epsilon}$ controls the rate of the coupling strengths adjustment. Since $\hat{\epsilon} \ll \epsilon$ such adjustments do not significantly slow down the operation of the simulator as they have to be performed much more rarely than adjustments of the gain. Equation (9) indicates that the couplings need to be reconfigured depending on the injection rate: if the coupling strength scaled by the gain at time t is lower (higher) than the objective coupling J_{ij} , it has to be increased (decreased). We have verified that Eqs. (5, 8, 9) find not just the value of the global minimum of the XY Hamiltonian for a variety of couplings and sizes of the system, but also the minimizers as Figs. 1b,c show.

To illustrate the implementation of the density and coupling adjustments and, therefore, realisation of the global minimum of the XY model by the actual physical system, we apply the developed algorithm to the square lattice of polariton condensates experimentally achieved in our previous work [11]. The required implementation of feedbacks for the density

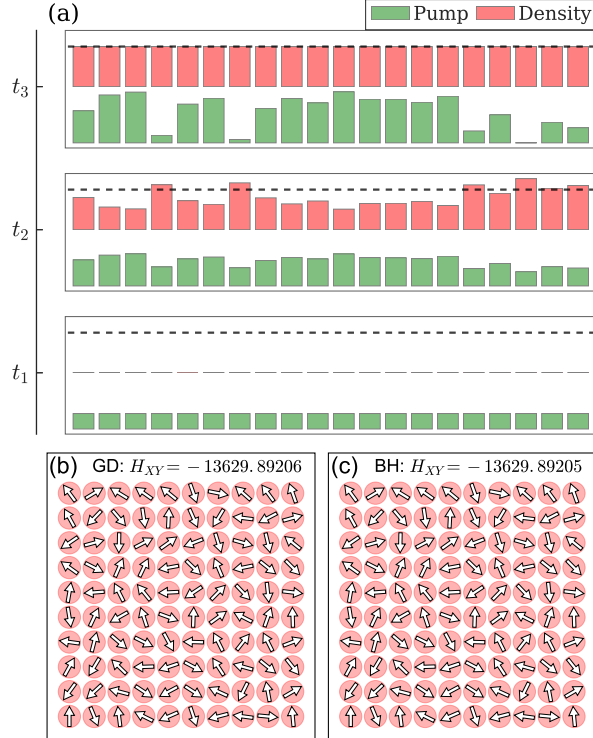


FIG. 1: (a) The schematics of operation of the GD simulator. Initially, at $t = t_1$ all CCs are equally pumped (green bars) below the threshold, and all have negligible number densities. As the pumping intensities increase and depending on the connectivity between CCs, the different CCs emerge (red bars) with different number densities as shown at some $t = t_2$. The individual control of the pumping intensity as described by Eq. (8) leads to the steady state with all the densities reaching the threshold at $t = t_3$. (b-c) The spin configurations of the absolute minimum of XY Hamiltonian for $N = 100$ CCs found by (b) numerical evolution of Eqs. (5,8,9) as described in the main text and (c) by the basin-hopping global optimization algorithm [27]. All spins are coupled with all the other spins with the coupling strengths that are randomly distributed in $[-10, 10]$. The values of the objective functions agree to 10 significant digits between two different methods.

(Eq. 8) and coupling (Eq. 9) adjustments can be experimentally achieved by adjusting the injection rates and reconfiguring the lattice geometry using the SLM. Liquid crystal based SLMs are widely used to generate arbitrarily structured beams of various intensity in optical micro-manipulation devices. We have already demonstrated the ease of using such SLMs for changing the coupling intensities in polariton graphs [11]. An alternative beam shaping technology is based on the digital micro-mirror devices that are capable of much faster switching rates for spatially controllable intensity (in excess of 20kHz whereas liquid crystal based SLMs are typically limited by a switching rate on the order of ~ 100 Hz due to the viscosity of the liquid crystal [26]). Therefore, the proposed feedbacks are well within

the technological capabilities of our platform. Figure 2a shows the density profile of 45 polariton condensates that interact by the outflow of the particles from neighbouring CCs. All CCs are equally pumped (with, say, $\gamma^{\text{inj}} \equiv \gamma_i^{\text{inj}}$) and, therefore, the CCs away from the margins have the largest occupation – they are fed by the particles coming from the eight neighbours. The CCs at the margins have the lowest occupation as they interact with only four or five neighbours. Such density heterogeneity between the lattice sites is clearly seen on Fig. 2a with the condensates on the margins being barely visible. The resulting configuration realises the global minimum of the XY model, but with the coupling strengths between i -th and j -th condensates given by $2\gamma^{\text{inj}}K_{ij}\sqrt{\rho_i\rho_j}$ with number densities ρ_i and ρ_j that are not known before the system reaches the configuration shown in Fig. 2a. The numerical simulation of the 7×7 polariton lattice shows not only the density variation between the sites in agreement with the experimental result but indicates the formation of a spin wave state (Fig. 2b) which manifests the presence of various couplings in the lattice. To realise the global minimum of the XY model for the given couplings (J_{ij}) we need to implement the feedback mechanisms described above and that we illustrate step by step. First, we remove the density heterogeneity by adjusting the gain mechanism described by Eq. (8). The resulting pumping profile is shown in Fig. 2c with the corresponding steady state number densities and phases in Fig. 2d. The spin wave in the presence of equal densities between the lattice sites is due to the different pumping intensities, and therefore, different couplings $\Delta_{ij}K_{ij}$ between the CCs across the lattice. We adjust K_{ij} according to Eq. (9) by changing the distances between the sites as Fig. 2e illustrates. The final steady state has equal densities and equal antiferromagnetic coupling strength between the nearest neighbours with phases alternating between 0 and π to give the expected global minimum of the XY model.

The developed procedure for the dynamical adjustment of the gain and coupling strengths, which is reflected in Eqs. (5,8,9) could be simulated by a classical computer and lead to a new class of global optimisation algorithms as we explore elsewhere [28] in particular, analysing if or when the actual physical gain-dissipative simulator can outperform the classical computer algorithm due to inherent parallelism of spanning various phases before the configuration that enables coherence at the threshold is reached and whether quantum superpositions contribute to processing of the phase configurations. These results can also be extended to other spin Hamiltonians such as the Ising and Potts [29].

In this paper we discussed gain-dissipative systems such as OPOs, optical cavities, lasers, and non-equilibrium condensates. The physics of the gain-dissipative oscillators may cover a much large variety of systems such as electronic circuits, voltage controlled oscillators,

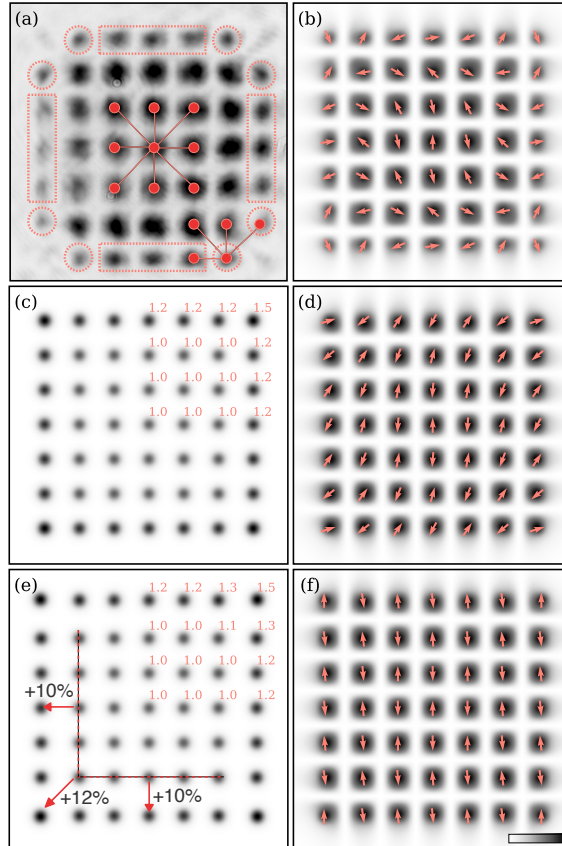


FIG. 2: (a) Contour plot of the number density of the polariton condensates formed by non-resonantly pumping polaritons with equal intensities (reproduced with permission from [11]). The distance between the neighbours is such that the coupling strength is antiferromagnetic for a polariton dyad with such separation at the condensation threshold. Red lines show the particle fluxes between the sites: the central site experiences the inflow of the particles from eight neighbouring sites whereas the sites on margins have only four or five neighbours. Dashed figures embrace the condensates with densities lower than the central condensates. (b,d,f) Contour plots of the steady state number density function $\rho = \int |\psi|^2 d\mathbf{r}$ obtained by the numerical integration of the full dynamical governing equations for 7×7 lattice and for the parameters used previously [11]. The lattice constant is $7.5\mu m$. (c,e) Contour plots of the pumping profiles at the steady state. Panels (c,d) were obtained by applying the density adjustments according to Eq. (8). Panels (e,f) were obtained by applying both the density adjustments and coupling adjustments according to Eq. (8) and Eq. (9). The resulting pumping intensities at the lattice sites are indicated for the top right quarter of (c,e) as the factor of the pumping at the lattice centre. The coupling strength adjustments are achieved by shifting the lattice sites as shown in red for the bottom left corner only in (e). Figure 2(a) reprinted with permission from [11]. Published in Nature Materials, Copyright (2017). <https://doi.org/10.1038/nmat4971>.

microelectromechanical systems, spin-torque nano-oscillators, oxide-based oscillators, etc. Our analysis is applicable to a broad family of oscillatory networks regardless of the nature of each oscillator as long as it is governed by the generic Eqs. (5), can be operated stably at the threshold and allows for the feedback mechanism of adjusting the pumping intensity of an individual CCs and their coupling strengths, similar to the operation of the considered systems.

NGB acknowledges financial support from the NGP MIT-Skoltech. K.P.K. acknowledges the financial support from Cambridge Trust and EPSRC.

-
- [1] Cuevas, G. D. & Cubitt, T. S. Simple universal models capture all classical spin physics. *Science* **351**, 1180 (2016).
 - [2] Aaronson, S. NP-complete problems and physical reality, *ACM SIGACT News*, **36**, 30-52 (2005)
 - [3] Zhang, S. & Huang, Y. Complex quadratic optimization and semidefinite programming. *SIAM J. Optim.* **16**, 871 (2006).
 - [4] Papadimitriou, C. H. & Yannakakis, M. Optimization, approximation, and complexity classes. *J. Comput. Syst. Sci.* **43(3)**, 425440 (1991).
 - [5] Utsunomiya, S., Takata, K. & Yamamoto, Y. Mapping of Ising models onto injection-locked laser systems. *Opt. Express* **19**, 18091(2011).
 - [6] Marandi, A., Wang, Z., Takata, K., Byer, R.L. & Yamamoto, Y. Network of time-multiplexed optical parametric oscillators as a coherent Ising machine. *Nat. Phot.* **8**, 937-942 (2014).
 - [7] Inagaki, T. *et al.* Large-scale Ising spin network based on degenerate optical parametric oscillators. *Nature Photonics* **10**, 415-419 (2016).
 - [8] McMahon, P.L. *et al.* A fully programmable 100-spin coherent Ising machine with all-to-all connections. *Science* **354**, 614-617 (2016).
 - [9] Takeda, Y. *et al.* Boltzmann sampling for an XY model using a non-degenerate optical parametric oscillator network. *Quantum Science and Technology* **3(1)**, 014004 (2017).
 - [10] Nixon, M., Ronen, E., Friesem, A. A. & Davidson, N. Observing geometric frustration with thousands of coupled lasers. *Phys. Rev. Lett.* **110**, 184102 (2013).
 - [11] Berloff, N. G. *et al.* Realizing the classical XY Hamiltonian in polariton simulators. *Nat. Mat.*

- 16(11)**, 1120 (2017).
- [12] Dung, D. *et al.* Variable potentials for thermalized light and coupled condensates. *Nat. Phot.* **11(9)**, 565 (2017).
- [13] Ohadi, H., R. L. Gregory, T. Freearge, Y. G. Rubo, A. V. Kavokin, N. G. Berloff, and P. G. Lagoudakis, "Nontrivial phase coupling in polariton multiplets," *Phys. Rev. X* **6**, 031032 (2016)
- [14] Leleu, T. *et al.* Combinatorial optimization using dynamical phase transitions in driven-dissipative systems. *Phys. Rev. E* **95**, 022118 (2017).
- [15] Oliva, R. A., & Strogatz, S. H. Dynamics of a large array of globally coupled lasers with distributed frequencies. *International journal of Bifurcation and Chaos* **11(09)**, 2359-2374 (2001).
- [16] Keeling, J. & Berloff, N. G. Spontaneous rotating vortex lattices in a pumped decaying condensate. *Physical review letters* **100(25)**, 250401 (2008).
- [17] Wouters, M. & Carusotto, I. Excitations in a nonequilibrium Bose–Einstein condensate of exciton polaritons. *Phys. Rev. Lett.* **99**, 140402 (2007).
- [18] Sigurdsson, H., Liew, T. C., & Shelykh, I. A. Parity solitons in nonresonantly driven-dissipative condensate channels. *Physical Review B* **96(20)**, 205406 (2017).
- [19] Carusotto, I. and Ciuti, C., Quantum fluids of light, *Rev. Mod. Phys.* **85**, 299 (2013)
- [20] Keeling, J. and Berloff, N.G. Exciton-polariton condensation. *Contemporary Physics* **52** (2011)
- [21] Lagoudakis, P. G. & Berloff, N. G. A polariton graph simulator. *New J. Phys.* **19**, 125008 (2017).
- [22] Kalinin, K. P., Lagoudakis, P. G., & Berloff, N. G. Matter wave coupling of spatially separated and unequally pumped polariton condensates. *Physical Review B* **97(9)**, 094512 (2018).
- [23] Acebrón, J. A., et al. The Kuramoto model: A simple paradigm for synchronization phenomena. *Rev. Mod. Phys.*, **77**, 137 (2005).
- [24] Kourtchatov, S. Y., Likhanskii, V. V., Napartovich, A. P., Arecchi, F. T., & Lapucci, A. Theory of phase locking of globally coupled laser arrays. *Physical Review A* **52(5)**, 4089 (1995).
- [25] Kozyreff, G. *et al.* Global coupling with time delay in an array of semiconductor lasers. *Phys. Rev. Letts* **85**, 3809 (2000).
- [26] Phillips, D. B. et al. Adaptive foveated single-pixel imaging with dynamic supersampling.

Science Advances, **3**, (2017)

- [27] Wales, D. J., & Doye, J. P. Global optimization by basin-hopping and the lowest energy structures of Lennard-Jones clusters containing up to 110 atoms. *J. Phys. Chem. A* **101(28)**, 5111-5116 (1997).
- [28] K.P.Kalinin & N.G.Berloff. Global optimization of spin Hamiltonians with gain-dissipative algorithms. *arXiv:1807.00699* (2018).
- [29] K.P.Kalinin & N.G.Berloff. Simulating Ising and Potts models and external fields with non-equilibrium condensates. *arXiv:1806.11457* (2018).
- [30] Suchomel, H. *et al.* An electrically pumped polaritonic lattice simulator. *arXiv:1803.08306* (2018)